Review Article on Advanced Imaging in The Diagnosis of Cardiovascular Diseases

Carotid plaque imaging and the risk of atherosclerotic cardiovascular disease

Guangming Zhu[1], Jason Hom[2], Ying Li[1,3], Bin Jiang[1], Fatima Rodriguez[4], Dominik Fleischmann[5], David Saloner[6], Michele Porcu[7], Yanrong Zhang[1], Luca Saba[7], Max Wintermark[1]

[1]Department of Radiology, Neuroradiology Section, [2]Department of Medicine, Stanford University School of Medicine, Palo Alto, CA, USA; [3]Clinical Medical Research Center, Luye Pharma Group Ltd., Beijing 100000, China; [4]Division of Cardiovascular Medicine and the Cardiovascular Institute, Stanford University, Palo Alto, CA, USA; [5]Department of Radiology, Cardiovascular Imaging Section, Stanford University School of Medicine, Palo Alto, CA, USA; [6]Department of Radiology, University of California San Francisco, San Francisco, CA, USA; [7]Dipartimento di Radiologia, Azienda Ospedaliero Universitaria di Cagliari, Cagliari, Italy

Contributions: (I) Conception and design: M Wintermark, J Hom, F Rodriguez, D Saloner, L Saba; (II) Administrative support: None; (III) Provision of study materials or patients: None; (IV) Collection and assembly of data: G Zhu, Y Li, B Jiang; (V) Data analysis and interpretation: J Hom, Y Zhang, M Porcu; (VI) Manuscript writing: All authors; (VII) Final approval of manuscript: All authors.

Correspondence to: Max Wintermark, MD, MAS. Department of Radiology, Neuroradiology Section, Stanford University School of Medicine, Palo Alto, CA, USA. Email: mwinterm@stanford.edu; Jason Hom, MD. Department of Medicine, Stanford University School of Medicine, Palo Alto, CA, USA. Email: jasonhom@stanford.edu.

Abstract: Carotid artery plaque is a measure of atherosclerosis and is associated with future risk of atherosclerotic cardiovascular disease (ASCVD), which encompasses coronary, cerebrovascular, and peripheral arterial diseases. With advanced imaging techniques, computerized tomography (CT) and magnetic resonance imaging (MRI) have shown their potential superiority to routine ultrasound to detect features of carotid plaque vulnerability, such as intraplaque hemorrhage (IPH), lipid-rich necrotic core (LRNC), fibrous cap (FC), and calcification. The correlation between imaging features and histological changes of carotid plaques has been investigated. Imaging of carotid features has been used to predict the risk of cardiovascular events. Other techniques such as nuclear imaging and intra-vascular ultrasound (IVUS) have also been proposed to better understand the vulnerable carotid plaque features. In this article, we review the studies of imaging specific carotid plaque components and their correlation with risk scores.

Keywords: Radiology; carotid plaque; risk score; atherosclerotic cardiovascular disease (ASCVD)

Submitted Jan 23, 2020. Accepted for publication Mar 17, 2020.
doi: 10.21037/cdt.2020.03.10
View this article at: http://dx.doi.org/10.21037/cdt.2020.03.10

Introduction

Atherosclerosis is the main pathophysiological process responsible for atherosclerotic cardiovascular disease (ASCVD), such as coronary, cerebrovascular, and peripheral arterial diseases (1). Cervical internal carotid artery plaque, most commonly occurring at the carotid bifurcation, is not only a marker for carotid atherosclerosis, but also a risk predictor of future ischemic events. Increasing data suggest that the presence of carotid plaque features of instability is associated with coronary and stroke events (2,3), highlighting the systemic nature of atherosclerosis, and the potential for unstable plaque detection in one territory to inform about disease status in other vascular beds. Carotid plaque is conventionally indirectly identified on the basis of measurements of luminal stenosis. With the rapid advances of structural vascular imaging, many additional morphological features of carotid plaques, including intraplaque hemorrhage (IPH), lipid-rich necrotic core (LRNC), fibrous cap (FC), calcification, and even neovascularization, can be identified and quantified.

The diagnosis of carotid atherosclerotic plaque has

shifted from pure stenosis quantification to plaque characterization, which allows for an improved pathophysiological understanding, and for more precise patient risk stratification and management (4). A recent meta-analysis indicated that IPH is common in patients with both symptomatic and asymptomatic carotid plaques and is a stronger predictor of stroke than any known clinical risk factors (5). Researchers and clinicians now have many imaging modalities available that allow for in-depth exploration of carotid artery plaque and its components. As the primary noninvasive imaging modality, Doppler ultrasound (US) can detect, grade, and monitor carotid plaque for many years, due to its high sensitivity and specificity, relatively low cost and lack of radiation (6). However, its performance is operator dependent and can be limited by the presence of calcification. computerized tomography (CT) and magnetic resonance imaging (MRI) can improve identification of many plaque features associated with vulnerability. Nuclear medicine and molecular imaging provide a promising prospect to further explore markers of plaque vulnerability, including inflammation and neovascularization. In 2018, the ASNR Vessel Wall Imaging Study Group published guidelines that focused on the implications and effects of technologies for carotid plaque imaging (4).

This review will focus on the techniques available to image carotid plaque and describe how certain modalities are well suited for assessing specific carotid plaque components. We will also illustrate the risk scores based on carotid plaque imaging and their ability to guide patient management.

Carotid plaque imaging

Carotid luminal imaging: focus on surface morphology

Luminal imaging is the traditional imaging method to evaluate the vascular caliber and plaque surface morphology. The degree of luminal stenosis has long served as the primary criterion for risk stratification of patients and for treatment decision-making, based on the results of randomized studies such as the European Carotid Surgery Trial (ECST) and North American Symptomatic Endarterectomy Trial (NASET). Luminal narrowing can be visualized and quantified by US, computed tomography angiography (CTA), magnetic resonance angiography (MRA), or catheter digital subtraction angiography (DSA). Catheter DSA has superior spatial and temporal resolution, when compared to other non-invasive, cross-sectional imaging modalities. Using DSA as the reference standard, Anzidei *et al.* compared the diagnostic performance of US, MRA and CTA. The results of this study (using a blood pool Gd-based contrast agent) indicate that CTA is the most accurate technique for evaluating carotid stenosis, with a slightly better performance than MRA (97% *vs.* 95% for steady state MRA and 92% for first pass MRA) and a greater accuracy than US (97% *vs.* 76%) (7). The surface morphology of carotid plaque is also considered a risk feature for stroke and cardiovascular disease (CVD). Surface irregularities and ulcerations represent an important sign of vulnerability. The ability of US to characterize surface morphology may be limited because of the acoustic shadowing of calcified components (8). The diagnostic accuracy with both contrast CT and MRI for detecting ulcers is superior to that of US (9,10).

However, luminal imaging can only provide limited information about the health of the vessel. Vulnerable carotid plaque lesions are often associated with minimal luminal stenosis because of positive remodeling (11). In the past two decades, several landmark clinical trials have demonstrated that the risk of an ischemic event with medical therapy alone in patients with mild-to-moderate stenosis was still considerable at about 20% over 5 years, which highlights the limitations of luminal imaging-based risk assessment (12,13). Histopathologic studies also demonstrated considerable differences between plaques with identical degrees of stenosis, and certain plaque features are associated with an increased risk of ischemic events (14). Therefore, assessment and understanding of the carotid plaque characteristics through high spatial resolution vessel wall imaging techniques, are regarded to be essential to understand the vascular risk in patients with carotid artery disease.

Carotid artery wall imaging

In contrast to carotid luminal imaging techniques, that represent the "effect" of the plaque and it is considered an indirect parameter, vessel wall imaging allows for the visualization of carotid plaque morphology and composition directly, and even for the assessment of pathological activity at the cellular level. Certain carotid plaque imaging characteristics are associated with an increased risk of ischemic events, independent of luminal stenosis. In general, the aim of vessel wall imaging is to look beyond the lumen and to identify those imaging features associated with

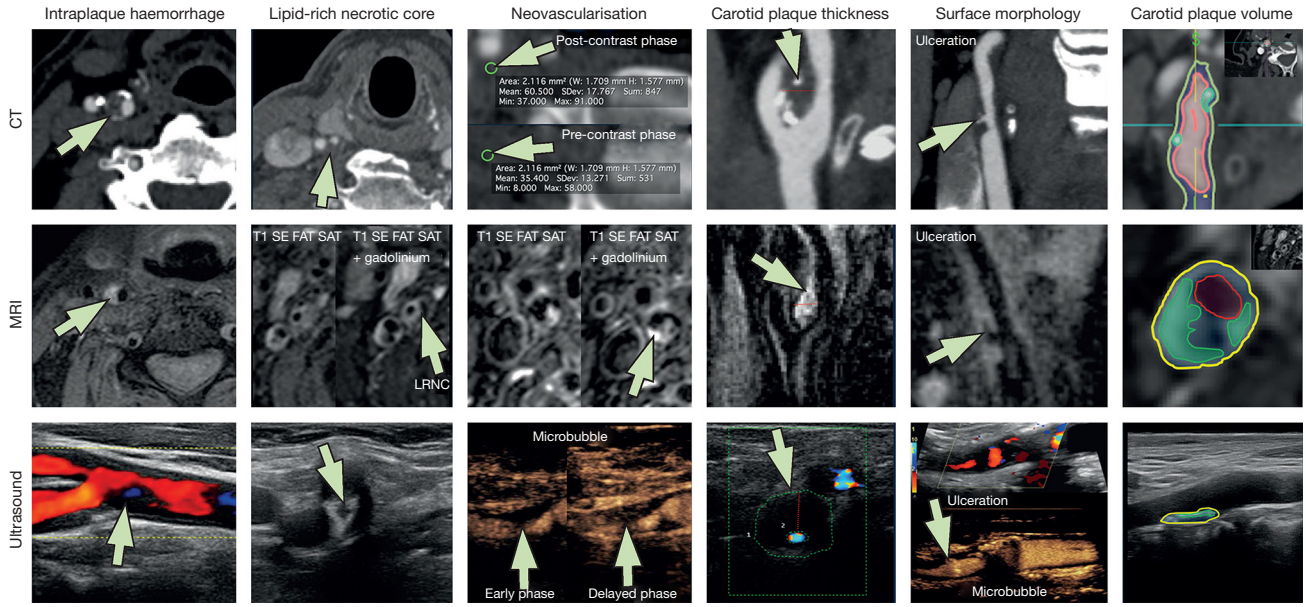

Figure 1 Imaging features of plaque vulnerability. Six features of carotid plaque vulnerability are shown in columns, and images were obtained by CT (upper row), MRI on a 3 Tesla scanner (middle row), and ultrasound (lower row). On ultrasound images, red colour indicates orthograde flow and blue colour shows retrograde flow. In the first column (intraplaque haemorrhage) and second column (LRNC), the arrow points to the feature detected. In the third column (neovascularisation), the arrows and green circles in the pre-contrast and post-contrast CT images (upper row) show how Hounsfield units increase after administration of contrast material. Similarly, in the MRI panel (middle row), after gadolinium contrast, the plaque (arrow) shows a significant increase in signal intensity because of enhancement of the plaque. The ultrasound images (lower row) show significant enhancement in the plaque (arrow) because of the presence of microbubble. Early phase is after 30 s and delayed phase is after 120 s. In the fourth column (carotid plaque thickness), the arrows indicate the plaque and the red dotted lines show the thickness of the plaque. The green dotted line in the ultrasound image represents the outer lumen of the plaque. In the fifth column (surface morphology), the arrows in all images show the ulcer. In the ultrasound images, the two panels show the difference in sensitivity using conventional B-mode colour Doppler and microbubble injection. In this case, the ulcer is visible only with the microbubble technique. The sixth column shows carotid plaque volume analysis and tissue segmentation. The red line shows the inner boundaries of the carotid plaque wall; the yellow line shows the outer boundary of the carotid plaque wall; the green colour represents the fatty component; the blue colour indicates the mixed component. CT, computerized tomography; MRI, magnetic resonance imaging; IPH, intraplaque haemorrhage; LRNC, lipid-rich necrotic core. T1 SE FAT SAT, T1 spin-echo fat saturation MRI sequence. [request copyright permission from Saba *et al.* (18)].

plaque vulnerability that are best suited for risk prediction.

US is the most widely available noninvasive imaging modality for real-time assessment of carotid plaque morphology. Meta-analyses highlighted the evidence using US in risk evaluation of patients with both asymptomatic and symptomatic carotid plaques (15,16). Newer generation technologies such as contrast-enhanced (CE) US (CEUS) and three-dimensional (3D) US provide extensive information about carotid plaque morphology. Due to its high signal-to-noise ratio (SNR), MRI has been the most popular imaging method for assessing carotid plaque features. When compared to histological gold standards, MRI demonstrated moderate-to-good sensitivity and specificity in detecting calcification, FC, IPH and LRNC, based on a meta-analysis including 17 studies (17).

CTA is a rapid imaging modality to detect carotid artery stenosis, and new studies indicate that vulnerable plaque features can be detected using CTA. CTA, particularly when dual-energy CT is used, is also very accurate in detecting carotid plaque calcifications (4). The imaging features of plaque vulnerability on US, MRI, and CTA are illustrated on *Figure 1*.

Positron emission tomography (PET) is one of the "molecular" imaging techniques that are used to

characterize the biological activity of atherosclerotic lesions, such as increased glycolytic activity and microcalcification.

In summary, among the noninvasive carotid wall imaging techniques, MRI still holds the greatest promise for evaluation of the risk features of carotid plaques because MRI has the greatest ability to detect low-contrast soft tissue abnormalities. Plaque features linked to vulnerability, such as plaque volume, IPH, LRNC, fissured FC and inflammation, will now be reviewed in the following sections. Selected studies on the compositions of carotid plaque and corresponding imaging findings are listed on *Tables 1*,*2*.

Table 1 Selected studies on the compositions of carotid plaque

Year	Author	Patients	Study size	Imaging modality	Target composition	Comparison	Main conclusion
2004	Kampschulte *et al.* (19)	Underwent CEA	26	MRI	IPH	Histologic analysis	MRI can detect and differentiate IPH with sensitivity and specificity of 96% and 82%
2006	Takaya *et al.* (20)	Consecutive subjects with asymptomatic 50–79% carotid stenosis	154	MRI	IPH, LRNC, FC	Ischemic events	Subsequent cerebrovascular events were associated with IPH (HR =5.2) and LRNC (HR for 10% increase =1.6)
2008	Wintermark *et al.* (21)	Underwent CEA	8	CTA	IPH, LRNC, FC	Histologic analysis	Good correlation with histologic examination for LRNC (κ=0.796) and IPH (κ=0.712)
2008	Yim *et al.* (22)	Consecutive subjects with carotid stenosis >70% on US	135	MRI-TOF	IPH	Histologic analysis	High signal intensity halo sign on MRI TOF is a marker of a fresh or recent IPH with high sensitivity and specificity (91% and 83%).
2009	Ajduk *et al.* (23)	Consecutive subjects with carotid plaques	31	CTA	IPH	Histologic analysis	Threshold of 31 HU for IPH has sensitivity and specificity of 100% and 64.7%
2009	Singh *et al.* (24)	50–70% asymptomatic carotid stenosis	91	MRI	IPH	Cerebrovascular events	IPH on carotid MRI is associated with cerebrovascular events (HR =3.59)
2009	Ota *et al.* (25)	Carotid stenosis >50% on US	77	MRI	IPH, LRNC, FC,	FC status	IPH and LRNC are associated with worse FC status
2010	U-King-Im *et al.* (26)	Consecutive patients with carotid MRI and CTA	167	CTA	IPH	MRI-defined IPH	Mean CTA plaque density cannot predict MRI-defined IPH due to significant overlap
2013	Saam *et al.* (27)	Meta-analysis	689	MRI	IPH	Ischemic events	IPH on MRI predicts cerebrovascular events (HR =5.69)
2013	Kwee *et al.* (28)	TIA/stroke subjects with 30–69% carotid stenosis	126	MRI	IPH, LRNC, FC	Recurrent cerebrovascular ischemic events	Recurrence of cerebrovascular ischemic events is associated with MRI-depicted LRNC (HR =3.200), thin/ruptured FC (HR =5.756), and IPH (HR =3.542)
2013	Gupta *et al.* (29)	Meta-analysis	779	MRI	IPH, LRNC, FC	Recurrent cerebrovascular ischemic events	Recurrence of cerebrovascular ischemic events is associated with MRI-depicted LRNC (HR =3.00), thin/ruptured FC (HR =5.93), and IPH (HR =4.59)

Table 1 (*continued*)

Table 1 (*continued*)

Year	Author	Patients	Study size	Imaging modality	Target composition	Comparison	Main conclusion
2014	Xu *et al.* (30)	Asymptomatic subjects with 50–79% carotid stenosis	120	MRI	IPH, LRNC	CAS	Development of new IPH is not associated with CAS
2016	Selwaness *et al.* (31)	Population-based Rotterdam study	1,731	MRI	IPH, LRNC, calcification	Ischemic events	IPH is associated with ischemic stroke in men (OR =2.39)
2017	Wang *et al.* (32)	With recent cerebrovascular events	31	MRI	IPH	Asymptomatic carotid side	Symptomatic side with stronger T1 signals, larger LRNC, and longer plaque length
2018	Saba *et al.* (33)	Underwent CEA	91	CTA	IPH, FC, LRNC	Histologic analysis	Threshold of 25 HU for IPH has sensitivity and specificity of 93.22% and 92.73%
2018	Brinjikji *et al.* (34)	Consecutive carotid artery disease subjects	38	MRI	IPH, LRNC, FC	MRI with surface coil	MRI with neurovascular coil has high sensitivity and specificity in identifying IPH (91.1%, 87.0%,) and LRNC (73.3%, 85.7%)
2019	Saba *et al.* (35)	Consecutive subjects with carotid CTA	123	CTA	IPH, LRNC	Ischemic events	The ratio of IPH/LRNC is associated with cerebrovascular events (AUC =0.811)
2002	Walker *et al.* (36)	Underwent CEA	55	CTA	LRNC	Histologic analysis	Analysis of plaque attenuation with single-slice spiral CT does not give useful information concerning plaque composition
2002	Wasserman *et al.* (37)	Consecutive subjects with carotid stenosis >30%	9	MRI	LRNC, FC, calcification	Histologic analysis	Contrast-enhanced MRI can discriminate FC from LRNC, as well or better than T2-weighted MRI
2005	Saam *et al.* (38)	Underwent CEA	31	MRI	LRNC, FC, calcification	Histologic analysis	MRI measurements of plaque composition are statistically equivalent to those of histology for LRNC (23.7 versus 20.3%) and FC (66.3% versus 64%)
2005	Cai *et al.* (39)	Underwent CEA	21	MRI	LRNC, FC	Histologic analysis	Good correlation between MRI and histology for length of the intact FC (r=0.73 and 0.80), and LRNC area (r=0.87)
2006	De Weert *et al.* (40)	Symptomatic carotid stenosis	15	CTA	LRNC, FC, calcification	Histologic analysis	MDCT can quantify calcification and FC in good correlation with histology (R^2 >0.73), but not LRNC
2007	Touzé *et al.* (41)	Consecutive subjects with carotid stenosis (40–69%, or >60%)	85	MRI	LRNC, FC, calcification, IPH	Intra- and Inter-observers	Intraobserver and Interobserver agreements: calcifications (κ=0.70 and 0.74), LRNC (κ=0.69 and 0.58), IPH (κ=0.82 and 0.62), FC (κ=0.58 and 0.28/0.26)
2013	Sun *et al.* (42)	16–79% carotid artery stenosis and visible plaque on US	59	MRI	LRNC	Serial MRI	IPH have a major influence on LRNC progression, more than clinical characteristics

Table 1 (*continued*)

Table 1 (*continued*)

Year	Author	Patients	Study size	Imaging modality	Target composition	Comparison	Main conclusion
2018	Sheahan *et al.* (43)	Consecutive subjects suspected carotid atherosclerosis	31	CTA	LRNC, calcification	Histologic analysis	Software-aided measurements have high correlation and low bias when compared with histopathologic measures.
2000	Hatsukami *et al.* (44)	Underwent CEA	22	MRI	FC	Histologic analysis	High level of agreement (89%) between MRI and histological findings (κ=0.87)
2002	Yuan *et al.* (45)	Scheduled CEA	53	MRI	FC	Ischemic events	MRI-depicted ruptured FC is highly associated with recent TIA/stroke (OR =23), compared with intact thick FC
2009	Kwee *et al.* (46)	Symptomatic subject with 30–69% carotid stenosis	45	MRI	FC, LRNC	Intra- and Inter-observers	Good interobserver agreements (κ>0.60) and excellent intra-observer agreements (κ=0.86 and 0.96) for FC status
2010	DeMarco *et al.* (47)	Consecutive subjects with 50–99% carotid stenosis	97	MRI	FC, LRNC	Ipsilateral ischemic events	Thin/ruptured FC and LRNC are associated with ipsilateral ischemic events
2013	Trelles *et al.* (48)	Suspected TIA/stroke	51	CTA	Complicated plaque	MRI	Maximum soft plaque component thickness on CTA is a reliable indicator of a complicated plaque with high sensitivity and specificity (65% and 94%)
2017	Paprottka *et al.* (49)	Consecutive subjects with ischemic stroke and carotid plaque >2 mm	178	MRI	Calcified nodules (CN)	Risk factors and events	Prevalence of CN is associated with hypertension, hypercholesterolemia, and symptomatic arteries
2010	Staub. *et al.* (50)	With contras-enhanced carotid US	147	US	Neovascularization	Risk factors and ischemic events	Neovascularization associated with higher CVD (OR =4.7) and CVE (OR =4.0)
2016	Huang *et al.* (51)	Meta-analysis	197	CEUS	Neovascularization	Histologic/clinical diagnosis	For qualitative CEUS, sensitivity, specificity, and diagnostic OR are 0.80, 0.83, and 3.22. For quantitative CEUS, they are 0.77, 0.68, and 7.06
2012	Saba *et al.* (52)	Consecutive subjects with TIA/stroke	29	CTA	Neovascularization	Histologic analysis	Carotid plaque enhancement is associated with micro-vessel density and neovascularization
2012	Qiao *et al.* (53)	With known carotid plaque	47	MRI	Neovascularization, IPH	Cerebrovascular events	Recent ischemic events are associated with IPH (OR =10.18) and adventitial enhancement (OR =14.90 and 51.17)
2018	Chowdhury *et al.* (54)	Meta-analysis	539	PET/CT	Inflammation	Symptomatic disease	^{18}F-FDG uptake on PET/CT between symptomatic and asymptomatic disease has a standard mean difference of 0.94

CEA, carotid endarterectomy; MRI, magnetic resonance imaging; IPH, intraplaque hemorrhage; LRNC, lipid-rich necrotic core; FC, fibrous cap; TOF, time-of-flight; CTA, computed tomography angiography; HU, Hounsfield unit; HR, hazard ratio; US, ultrasound; TIA, transient ischaemic attack; CAS, carotid atherosclerosis score; OR, odds ratio; AUC, area under the curve; CT, computerized tomography; MDCT, multidetector-row CT; CEUS, contrast-enhanced US; FDG, fluorodeoxyglucose; PET, positron emission tomography.

Table 2 Common Imaging findings of carotid plaque components

Imaging modalities	IPH	LRNC	FC	Calcified nodules
MRI				
TOF	Hyper	Iso	Iso/Hypo	Hypo (white-blood)
T1	Hyper	Iso/hyper	Iso/Hypo	Hypo (black-blood)
T2	Variable	Hypo	Hypo	Hypo (black-blood)
CTA	Intermediate density	Low density	Intermediate density (hard to see)	High density
US	Hypo	Hypo	Hyper	–

IPH, intraplaque hemorrhage; LRNC, lipid-rich necrotic core; FC, fibrous cap; TOF, time-of-flight; CTA, computed tomography angiography; US, ultrasound.

Plaque thickness, volume and carotid plaque burden

The thickness and volume of the carotid plaque are quantifiable with US, CT, and MRI. A meta-analysis based on seven 3D US studies suggested good reproducibility for assessment of carotid plaque volume (55). Multiple studies have suggested plaque thickness or plaque volume to be more strongly associated with ischemic events than the degree of stenosis (56,57). Indeed, the carotid plaque burden is distinct from the severity of carotid stenosis or the plaque thickness (58). A meta-analysis confirmed that carotid total plaque area (TPA), a common measurement of carotid plaque burden, is superior to carotid intima-media thickness (IMT) in cardiovascular risk prediction (59). Another study also suggests carotid plaque burden is highly correlated with coronary calcium scores, whereas IMT is not (60).

Mean/maximum wall area and mean/maximum wall thickness are common measurements of carotid plaque burden. They can be obtained on cross-sectional images through segmenting lumen and total vessel area. Accurate segmentation requires clear delineation of lumen and outer wall boundaries, and therefore high image spatial resolution is required. CTA has good spatial resolution and has emerged as a useful tool in the assessment of carotid plaque burden and the volume of the sub-components of the plaque, according to the attenuation values of the voxels (61). Although the spatial resolution of MRI is lower than that of CT, MRI soft tissue contrast is far superior. Despite minor methodological differences, multiple studies have evaluated the precision and accuracy of carotid wall measurements by carotid MRI, with excellent inter-observer and inter-scan reproducibility (62-65). Luo *et al.* showed high agreement between *in vivo* MRI measurements of carotid plaque burden and corresponding *ex vivo* MRI measurements. The correlations between minimum lumen area, maximum wall area, and wall volume were weak, which may suggest these provide different information from carotid plaque burden (66). The measurement precision is influenced not only by image quality and spatial resolution, but also by the carotid plaque volume. Larger carotid plaques and wall area measurements are associated with smaller relative measurement errors (67).

IPH

IPH is one of the key features of vulnerable carotid plaques and contributes to rapid plaque progression (31,42). IPH is thought to be caused by plaque rupture or rupture of plaque neo-vessels. IPH may serve as a measure of risk for the development of future cardiovascular events (68,69). It is also considered the strongest imaging parameter associated with the future occurrence of stroke (27). A meta-analysis of 9 studies demonstrated carotid IPH by MRI to be associated with increased risk for future ischemic stroke in patients with symptomatic and asymptomatic carotid plaques [hazard ratio (HR) =4.59, 95% confidence interval (CI): 2.79–7.24] (29). Another meta-analysis of 689 patients suggested the event rate for cerebrovascular events in patients with MRI-visible IPH was 17.8% a year, compared to 2.4% in patients without MRI-visible IPH (27). Saba *et al.* demonstrated the plaque ipsilateral to the symptomatic side has significantly larger volume and a higher percentage of IPH compared with the contralateral, asymptomatic side (35). In asymptomatic individuals with 50–70% carotid stenosis, the presence of IPH on MRI was associated with a markedly increased risk of cerebrovascular events (HR =3.59, 95% CI: 2.48–4.71) (24).

US is less suitable methods for the detection of IPH. Due to the poor signal-to-noise and moderate spatial resolution,

it is difficult to distinguish IPH from LRNC on US. Many different studies used different Hounsfield unit (HU) thresholds on CTA to determine IPH. Ajduk *et al.* examined carotid plaques from 31 patients who underwent operations for carotid artery stenosis. They compared the preoperative multidetector-row CT analysis of carotid plaques with histological analysis. Using 33.8 HU as the IPH cutoff value, CTA had 100% sensitivity and 64.7–70.4% specificity to detect IPH (23). Saba *et al.* used a threshold of 25 HU and IPH presence was detected with a sensitivity of 93.2% and a specificity of 92.7%, compared with histopathological evaluation (33). But, in another comparison between carotid CTA and carotid endarterectomy (CEA) specimens for 8 patients with recent transient ischaemic attack (TIA), the results suggested a higher HU measurement of IPH with a cutoff value at 72 HU. This study also demonstrated significant overlap between HU measurements of IPH and fibrous tissue which limits the value of HU to determine various plaque components (21). Other authors have exploited indirect findings on carotid CTA to predict IPH. For example, a study suggested CTA plaque ulceration had high sensitivity (80.0% to 91.4%) and specificity (93.0% to 92.3%) for prediction of MRI-defined IPH (26). Eisenmenger *et al.* proposed a model, which includes rim sign, maximum soft plaque thickness, the North American Symptomatic Carotid Endarterectomy Trial (NASCET) stenosis, and ulceration, to predict IPH on CTA. A positive rim sign was defined as adventitial calcification (<2 mm thick) with internal soft plaque (>2 mm thickness). This model had excellent IPH prediction with area under the curve (AUC) =0.94 (70). But in general, accurate detection and quantification of IPH with carotid CTA is difficult because of the overlap in HU with soft tissue on one side and with calcium on the other side.

IPH can be optimally evaluated on MRI T1-weighted and fat-/flow-suppressed sequence as hemoglobin products induce T1 shortening (71) (*Figure 1*). In a study of 26 patients undergoing time-of-flight (TOF) and T1- and T2-weighted imaging prior to endarterectomy, MRI was able to differentiate IPH from juxta-luminal hemorrhage with near 100% accuracy (19). High-resolution MRI black-blood techniques can provide good blood suppression and high resolution (17). Black-blood sequences using T1-weighted imaging with fat saturation or magnetization prepared rapid acquisition gradient echo (MPRAGE) sequences demonstrate IPH as T1 hyperintense with signal intensities at least 50% higher than sternocleidomastoid muscle (72). The sensitivity of IPH identification using surface coils is about 98% compared to the histological gold standard (73). However, carotid plaque protocols using surface coils have not been integrated into standard clinical practice, because carotid surface coils are not widely available, and have small coverage. Indeed, the detection of IPH could also be achieved at lower spatial resolution using large neck coils with high sensitivity (91.1%) and specificity (87.0%), without the need for dedicated carotid surface coils (34). IPH signal intensities may change over time. MRI allows categorization of IPH into fresh (type 1), recent (type 2), and old (type 3) subtypes, but there is no evidence that the subtype of IPH makes a difference in terms of predicting future ischemic events (32). Fresh IPH is hyperintense on T1-weighted images (T1WIs) and hypointense/isointense on T2-weighted images (T2WIs) and proton density-weighted (PDW) images. Both IPH and LRNC may exhibit high T1 signal. They can be distinguished on T1-weighted TOF sequences, with IPH typically being hyperintense on both T1 and TOF (*Figure 1*). Recent IPH is hyperintense and older IPH is hypointense on all contrast weightings. Yim *et al.* demonstrated that recent IPH has a "halo sign" (a peripheral rim of high signal intensity around the carotid) on maximum intensity projection images of TOF MRI. This sign can last for months to years with a negative predictive value of 95% (22).

In summary, MRI is the best imaging technique for the detection of IPH because of the MRI characteristics of hemoglobin (74), which can be detected and characterized by multiple MRI sequences (*Figure 2*) (4).

LRNC

In carotid plaques, the LRNC is a heterogeneous combination of cholesterol crystals, debris of macrophages and inflammatory cells, and particles of calcium. A longitudinal MRI study of 120 asymptomatic individuals showed that carotid plaques with a percentage of LRNC greater than 40% were more likely to develop rupture of the FC over a 3-year follow-up (30). Vulnerable plaques are characterized by the presence of a thin FC covering a large LRNC. The LRNC size was found to be a strong predictor of FC disruption (25,30), which exposes the LRNC to luminal blood and then activates the thromboembolic cascade. Therefore, LRNC is another important risk factor of cerebrovascular events (20,28,29).

On B-mode US imaging, LRNC and IPH can both appear hypoechoic, also known as a juxta-luminal black area (JBA) (*Figure 1A*). A JBA of more than 8 mm^2 was associated with a high prevalence of symptomatic plaques

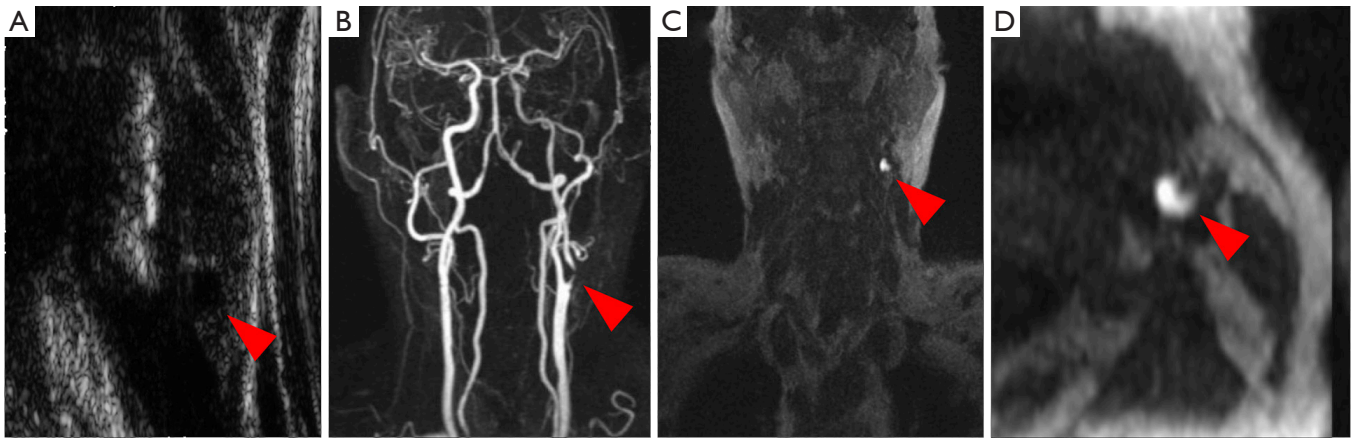

Figure 2 Imaging feature of IPH. Carotid ultrasound shows carotid plaque with significant ICA stenosis, and a hypoechoic are (A, arrowhead) which could represent either LRNC or IPH. Gadolinium-enhanced MRI confirms the left ICA stenosis (B, arrowhead). Within the plaque, hypersignal can be detected on the source, pre-contrast T1WIs for the MRA, which suggests IPH (C,D, arrowhead). IPH, intraplaque hemorrhage; ICA, internal carotid artery; LRNC, lipid-rich necrotic core; MRI, magnetic resonance imaging.

in all grades of stenosis and independently associated with neurological symptoms (75). Another study with 1,121 patients demonstrated the size of JBA on US images of asymptomatic carotid plaques to be predictive of the occurrence of stroke. The mean annual stroke rate was 0.4% with a JBA <4 mm^2, 1.4% with a JBA from 4 to 8 mm^2, 3.2% with a JBA 8 to 10 mm^2, and 5% with a JBA >10 mm^2 (P<0.001) (76). However, it is difficult to distinguish LRNC and IPH on US, which limited the role of US for the characterization of carotid plaque morphology.

Carotid CTA can detect lipid components because of the lipid-tissue attenuation properties. However, the use of simple HU to detect LRNC on carotid CTA has led to inconsistent results. Initial studies compared the detection of LRNC on CTA with histological evaluation of CEA specimens, which suggested a statistically significant decrease in HU density measurements with increasing plaque lipid, but with a high standard deviation of these values (36). The results suggest that the plaque attenuation on CTA provides only limited information regarding plaque composition, mostly because LRNC and IPH both show attenuation values less than 60 HU and are therefore hard to distinguish (48). Multiple studies demonstrate the association between low HU value in the plaque (<35 HU) and IPH, which may also include LRNC (23,33). There is also a significant overlap of HU measurements between fibrous tissue and LRNC (21). An additional potential confounding factor is the blooming effect of calcium on CTA. For example, de Weert *et al.* suggested a measured attenuation value of LRNC was 25±19 HU with a cutoff of 60 HU to differentiate between LRNC and fibrous tissue. But a good correlation of LRNC size measured on CTA compared with CEA specimen histology is only observed in mildly calcified carotid plaques (0–10%) (40). Sheahan *et al.* proposed a software algorithm which can mitigate the blurring and partial volume effect of routine CTA acquisitions. It produces accurate quantification of LRNC and calcium with a high correlation and low bias between the software analysis and histopathological quantitative measurements (43).

MRI is superior to CT for detection of the LRNC because LRNC typically appears hyperintense on T1WI and isointense on TOF images, which can be used to distinguish LRNC with IPH. LRNC can be detected as a focal hypointense region within the carotid vessel wall on T2WI and a focal non-enhancing region on CE T1WI (37,39). Lack of internal enhancement indicates LRNC, given the avascular nature of the core. LRNC can be best identified using a combination of T1 fat-saturated black blood imaging with and without contrast, where it appears as a hypointense/non-enhancing region. The presence of IPH within the LRNC may result in T2WI hyperintensity, which makes delineation of FC and LRNC difficult (37). MRI still remains the most promising tool of the day for LRNC with high accuracy, while combining multimodal MRI sequences.

FC

The FC is a layer of fibrous connective tissue that

separates the LRNC of the atherosclerotic plaque from the arterial lumen. The intact thick FC is associated with a low risk of plaque rupture, whereas a thin FC is associated with a mild risk, and a fissured FC with a high risk of plaque rupture (45,47). Histological studies indicate that a cap thickness <500 μm identifies ruptured plaques most reliably (77). Rupture of the FC exposes the thrombogenic LRNC to flowing blood, which may result in arterial thrombus formation and/or cerebral embolization.

The FC displays stronger echoes on conventional US than the overall plaque and blood. Integrated ultrasonic backscatter was found to be lower in a thin FC as compared with a thick FC (78). Overall however, the success of using conventional US to characterize the FC is limited (79), with a 73% sensitivity and 67% specificity using stratified gray-scale median (GSM) measurements (80). Intravascular US (IVUS) can provide real-time cross-sectional image acquisition of vessel wall and be used to define plaque morphology, such as LRNC, FC, and calcifications. IVUS historically was the gold standard for quantitative and qualitative evaluation of the vascular wall and lumen (81), but it is hard to incorporate in the standard clinical practice due to its invasiveness and higher costs.

Few studies have proposed using CT to detect the carotid plaque FC and those results have not been validated in a separate set of patients. For example, Wintermark *et al.* used an automated carotid plaque classification algorithm to identify the carotid plaque compositions. The results showed a good linear regression between CTA and histology examination for FC thickness (21). Saba *et al.* manually compared pre-contrast and post-contrast carotid CTA and then demonstrated both plaque neovascularization and fissured FC were associated with plaque enhancement (33). More studies and advanced techniques may help make the approach more suitable for clinical use in the future.

Because of MRI's limited spatial resolution, it is challenging to quantitatively measure the thickness of FC on carotid MRI. However, MRI is used to classify FCs as thick, thin, or ruptured. Thick FC shows up as a dark band on 3D TOF, between the lumen and the rest of the wall. On T2WIs and CE images, FC is distinguishable from the underlying LRNC and considered to be thick if it is readily visible. Ruptured FC is considered if there is juxta-luminal hyperintense signal on 3D TOF, which indicates the presence of fissure or ulceration. Although certain studies indicate that classification of FC by 3D TOF has a high agreement with histological findings (kappa =0.83) (44), other recent studies suggest poor reproducibility in identifying FCs by non-CE-MRI. According to Touzé *et al.*'s study, the Kappa values for the intra-observer reproducibility for the FC thickness on T2WI and TOF were 0.58 and 0.33, respectively, while the Kappa values for the inter-observer reproducibility were 0.28 and 0.26 (41). The reproducibility can be improved by using CE-MRI, because the FC enhances after intravenous administration of gadolinium-based contrast agents. Utilizing a multisequence MRI protocol with CE-MRI, Kwee *et al.* demonstrated a good interobserver (Kappa =0.60) and a very good intra-observer agreement (Kappa =0.86) for the assessment of the FC status of carotid artery plaques (46). Cai *et al.* also suggested that *in vivo* high-resolution CE-MRI is capable of quantitatively measuring the dimensions of the intact FC. Blinded comparison of corresponding MR images and histology slices showed moderate to good correlation for length ($r=0.73$, $P<0.001$) and area ($r=0.80$, $P<0.001$) of the intact FC (39).

In summary, due to the artifacts related to the edge blurring and halo effects, the assessment of FC using CT technique is limited. The application of IVUS is also limited because of its invasiveness and higher cost. MRI is the preferred technique to assess the FC, particularly with the use of gadolinium-based contrast agents (18).

Calcified nodules

The concept of the calcified nodule, first introduced by Virmani *et al.*, refers to a lesion with luminal thrombus associated with an eruptive, dense area of calcium and underlying calcific plaque (82). On carotid MR, calcified nodules show up as a convex shaped hypointense area on white-blood (TOF) and black-blood (T1W, PDW and T2W) images protruding into the lumen with a minimum diameter of 1 mm (38). These calcified nodules are more often present in older individuals and in patients with tortuous arteries. Calcified nodules were found in 7.9% of arteries and 14.5% of patients with carotid plaques ≥2 mm. The majority of calcified nodules are found at or near the carotid bifurcation. A prospective study based on MRI indicates the prevalence of calcified nodules to be significantly higher in symptomatic arteries, suggesting that calcified nodules may play a role in the pathogenesis of ischemic stroke in a subset of patients (49). Calcified nodules are known to cause 5% of coronary infarcts (11). About 6–7% of carotid thromboses are thought to be caused by calcified nodules, although this number is derived from a low number of cases (83).

Multidetector-row CTA (MDCTA) offers increased

spatial and temporal resolution and thus exhibits a potential for calcium detection and quantification. There are several studies using CTA to assess the role of carotid calcification. For example, Mosleh *et al.* assessed CTAs from acute stroke patients and demonstrated patients with speckled (<3 mm) and/or larger calcifications had a higher risk of cardiovascular events within 1 year (84). However, there is still no study focusing on calcified nodules on carotid CTA.

Inflammation, intraplaque neovascularization, and plaque metabolism

CTA has a higher sensitivity and specificity than MRI for the detection of arterial calcifications. While vascular wall calcifications may create artifacts that limit visualization of intraluminal flow and overestimate the degrees of stenosis, MRI improves visualization of heavily calcified arteries when compared to CTA.

Other important features of plaque vulnerability are inflammation and intraplaque neovascularization, both of which are associated with plaque metabolic activity (18). Plaque inflammation, predominantly in the form of T lymphocyte and macrophage infiltration, is closely associated with plaque rupture (85). Neovascularization has been described in the early stages of plaque development and may prevent hypoxia as the carotid wall thickens. However, it is also associated with IPH and plaque inflammation (86).

CEUS is a technique that utilizes an intravenous microbubble contrast agent to assess plaque and, in particular, neovascularization. After injection, intraplaque neo-vessels can be identified by the movement of microbubbles from the adventitia to the plaque core. A meta-analysis of 20 studies confirmed that plaque enhancement on CEUS was significantly associated with intraplaque neovascularization (51). Plaque enhancement is also markedly higher in symptomatic plaques and associated with increased cardiovascular events (50,87). Persistent plaque enhancement following contrast administration may reflect increased plaque infiltration by inflammatory cells (88).

Imaging plaque inflammation and neovascularization with carotid CT and MRI also requires intravenous administration of contrast agent. The amount of plaque contrast enhancement on CTA is associated with the extent of intraplaque neovascularization (52). Categorized by the degree of adventitial enhancement on CE-MRI, carotid plaque neovascularity was suggested to be independently associated with previous cerebrovascular ischemic events (53). Dynamic contrast enhancement perfusion MRI (DCE-MRI) measures changes of signal intensity in tissues over time (usually up to 5–10 min) after bolus administration of gadolinium and uses clinically available gadolinium contrast to study the amount and permeability of micro-vessels (89). Kerwin *et al.* developed a DCE-MRI protocol that was suitable to image plaque neovascularization quantitatively in carotid stenosis (90). Further histological validation showed that pharmacokinetic parameters extracted from DCE-MRI of carotid plaque are reliable indicators of not only plaque microvasculature but also macrophage content (91,92). However, due to the small size and motion of the vessel wall, the role of DCE-MRI to characterize plaque activity in the clinical setting is limited. Unlike DCE-MRI, which assesses inflammation indirectly, ultra-small superparamagnetic particles of iron oxide (USPIO)-enhanced MRI can target atherosclerotic plaque inflammation directly as USPIO particles are up-taken by macrophages via surface scavenger receptors. Areas with active macrophage infiltration appear hypointense on T2*-weighted images. In a study by Tang *et al.*, all symptomatic carotid arteries had inflammation, as evaluated by USPIO-enhanced imaging, while the contralateral side in patients with symptomatic carotid stenosis demonstrated inflammation in 95% of plaques, despite a mean stenosis of only 46% (93). Smits *et al.* demonstrated that there is no correlation between USPIO and fluorodeoxyglucose (FDG) uptake in carotid artery plaques, which may indicate that USPIO-MRI and ^{18}F-FDG-PET/CT visualize different pathophysiological processes related to plaque inflammation and may be complementary to identify vulnerable plaques (94). Larger studies are required to establish a clear role for USPIO-enhanced MRI beyond the research setting.

Plaque activity in carotid atherosclerotic plaques can be assessed using other molecular imaging techniques, such as PET/CT with ^{18}F-FDG as a commonly used tracer. Many studies have suggested the potential of ^{18}F-FDG PET to image and quantify plaque inflammation (95,96). In a recent meta-analysis of 14 studies with a combined total of 539 participants, Chowdhury *et al.* demonstrated increased ^{18}F-FDG activity of the culprit carotid plaque after an ischemic event (54). Another meta-analysis of seven studies with 287 participants indicated that statin treatment was associated with a significant reduction in arterial wall inflammation, based on ^{18}F-FDG PET-CT imaging evaluation (97). Other recent studies, however, show that ^{18}F-FDG uptake in the carotid plaque correlates with the risk of cardiovascular ischemic events, but fails to discriminate culprit from non-culprit lesions (98). Since there is still no consensus on the clinical role of ^{18}F-FDG

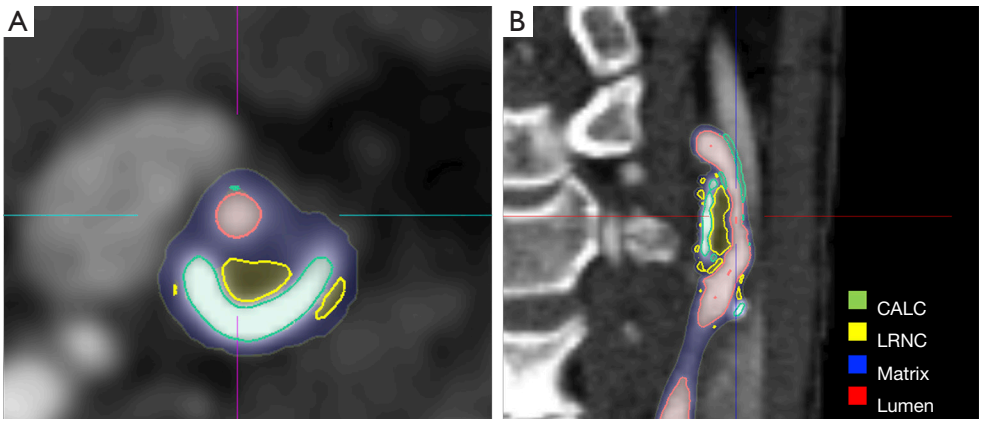

Figure 3 Semi-automatic segmentation and analysis of carotid plaques on CTA. Semi-automatic segmentation of the left carotid plaque in axial plane indicates the lumen (red), matrix (blue), LRNC (green), and CALC (yellow) (A). Cross-sectional representations of carotid plaque in coronal plane (B). CTA, computed tomography angiography; LRNC, lipid-rich necrotic core; CALC, calcification.

PET/CT to assess atherosclerotic plaque inflammation and to predict cardiovascular events, multicenter prospective studies are required (99). Other more inflammation-specific tracers, such as DOTATATE, 18-kDa translocator protein (TSPO) tracers, and ^{18}F-sodium florid (^{18}F-NaF), are also currently being investigated (100-102).

In general, although new imaging techniques, including CEUS, DCE-MRI, and PET/CT, have a lot of potential in the assessment of atherosclerosis, those modalities are still far from widespread clinical adoption. This is particularly true because these advanced imaging techniques require an increased level of protocol compliance for results to be accurate.

Carotid plaques imaging and new techniques

Since carotid vessel wall imaging may allow for more precise estimation of the vascular risk, a variety of new imaging modalities have been proposed over the last two decades for the identification of specific carotid plaque features. 3D US is a novel technique which has shown excellent specificity for the evaluation of stenosis and plaque volume (103). US elastography is an US technique which can quantify carotid plaque elasticity and intraplaque neovascularization (104). A recent study suggested that US elastography parameters, such as cumulated axial translation and the ratio of cumulated axial strain to cumulated axial translation, might be able to discriminate vulnerable carotid artery plaques from nonvulnerable plaques (105).

In the MRI arena, a new diffusion-weighted turbo spin echo sequence was developed in a pilot study, which demonstrated that *in vivo* apparent diffusion coefficient (ADC) values of LRNC were significantly lower than that of fibrous tissue (106). Other new techniques have also been developed to further improve the detection of IPH. Zhu *et al.* developed a 3D spoiled gradient-recalled echo sequence with inversion recovery and multiple echoes (3D SHINE) to detect and classify the IPHs based on T2* estimated from the multi-echo acquisition (107). Other new MRI techniques include SNAP imaging (simultaneous non-contrast angiography and IPH imaging) (108), MATCH (a 3D spoiled segmented fast low angle shot readout with 3 different contrast weightings acquired in an interleaved fashion) (109), and GOAL-SNAP (a high-resolution vessel wall T1 mapping technique by adopting efficient radial data acquisition and sliding window image reconstruction) (110).

A semi-automated approach for specific plaque features can be more reliable and less time-consuming. Several studies validated that a semi-automatic CTA-based image segmentation approach, using an imaging processing software package (*Figure 3*), can identify, locate, characterize and quantify atherosclerotic plaques in carotid artery (21,111-114). With the development of deep learning technology, artificial intelligence (AI) has also been proposed to automatically identify, classify, and quantify the carotid plaque composition. Lekadir *et al.* built a convolutional neural network (CNN) to extract from the images the information that is optimal for the identification of the different carotid plaque components, which showed a correlation of about 0.90 with the clinical assessment of

LRNC, FC, and calcified tissue areas (115). Many studies have applied AI for the optimization of image acquisition or utilization post-processing tools, especially for MRI. Coronary artery disease (CAD) risk stratification tools using machine learning and based on carotid artery imaging have been proposed, and the most recent studies have shown a cross-validation accuracy of more than 95% (116).The application of AI methods to carotid plaque imaging is still in its infancy and many innovations in this field are expected in the years to come (117).

ASCVD risk scores and carotid plaques imaging

ASCVD remains the leading cause of death globally (118,119). The Pooled Cohort Equations were developed in 2013 to predict the 10-year risk of ASCVD (120). Other calculators such as Framingham, QRISK-3, and Reynolds Risk Scores similarly include basic clinical features such as patient age, race, blood pressure, diabetes status, and lipid levels to predict both long- and short-term risk for an ASCVD event (121). These risk score calculators fail to consider plaque-specific features. Previous studies suggested only some concordance but not a perfect overlap between the 10-year ASCVD risk score and carotid artery imaging findings (122). All these calculators are population-based and may not be suitable for populations other than those they were developed in (121,123). For example, Gobardhan *et al.* suggested that asymptomatic South Asians with type 2 diabetes mellitus more frequently developed ASCVD compared to Caucasians despite similar risk prediction scores. Noting the limitations of risk prediction across minority groups, the contemporary U.S. 2018 multi-society lipid guidelines recommend caution in considering populations who were not included in the development of risk prediction algorithms (124). These guidelines also note that there are certain high-risk features, such as patient ethnicity, that should be considered when deciding on appropriate prevention strategies.

Coronary artery calcium (CAC) is one of the most studied imaging biomarkers in cardiovascular medicine. The MESA study showed that a CAC score of 0 can help lower estimated CVD risk (125). Per the most recent American Heart Association/American College of Cardiology (AHA/ACC) guidelines, CAC screening can be considered for intermediate risk populations (7.5% to 20% 10-year ASCVD risk score) when treatment decisions are uncertain (124).

However, the CAC score may not be effective for populations with low (<5%) and high (>20%) 10-year estimated ASCVD risk (126). In certain populations, carotid artery imaging biomarkers such as maximal plaque thickness, soft plaque, and ulceration, are more closely associated with the 10-year ASCVD risk score than the CAC score is (127). Recent US Preventative Services Task Force (USPSTF) guidelines highlight the fact that "CAC score testing showed no benefit over traditional CVD risk assessment in preventive medication use or risk factor control" (128). Adding CAC score to existing CVD risk assessment models can lead to a small improvement in discrimination and risk reclassification, but there have been no clinical trials to date showing that measuring CAC can improve cardiovascular outcomes.

An increasing number of studies have demonstrated the correlation between carotid plaque features and the risk of CVD (2,3,8,31,57,59,69,84,122,127,129-138). These studies highlight the potential for carotid plaque detection and characterization to inform about the atherosclerotic status in the coronary artery system. Several risk score systems based on or including carotid plaque status were developed. Khanna *et al.* proposed a risk calculator called AtheroEdge Composite Risk Score (AECRS1.0), which uses conventional cardiovascular risk factors along with five US image-based phenotypes, including IMT (Ave., Max., Min.), IMT variability, and TPA. AECRS1.0 has the best performance with an AUC of 0.990, compared to five other calculators, including FRS, UKPDS, and etc. (134). Another US image-based risk score system is the carotid plaque score, which is computed by summing the maximal thickness of plaques (132). It was evaluated by multiple studies in Japanese populations and was demonstrated to predict the atherosclerotic severity of coronary arteries (130-132,139). Tada *et al.* suggested that the carotid plaque score is a better marker to identify increased risk for recurrence of CVD, compared to the carotid IMT (131). However, in another multiethnic cohort, MESA, the CAC score had a better performance than the carotid plaque score in terms of prediction, discrimination, and reclassification of CVD and coronary heart disease (CHD) (132). Banchhor *et al.* have conducted several studies showing that calcium scoring is a stronger predictor of stenosis in patients with CVD (116).

Although many CT and MRI image-based marker were used to investigate the correlation between the carotid plaque features and the risk of CVD, there is still no risk score system based on CTA or multimodal MRI. Selected quantitative imaging carotid features extracted from CT carotid artery analysis might be able to predict the ASCVD

risk scores (114). However, approaches based on image markers are still investigational and not part of the clinical mainstream. Large prospective longitudinal studies are needed to build and validate imaging-based risk scores and their clinical usefulness.

Summary

In summary, rapid advances in noninvasive carotid artery imaging provide important pathophysiological insights. There is a growing body of evidence that supports use of carotid artery imaging to characterize carotid plaque features including carotid plaque burden, plaque composition, luminal surface condition, and plaque inflammation and neovascularization. Identification of these plaque features may further enhance current ASCVD risk stratification algorithms and, in turn, help guide preventive treatment decisions. The USPSTF has rigorously assessed whether incorporating the ankle-brachial index (ABI), high-sensitivity C-reactive protein (CRP) values or CAC scores into ASCVD risk assessment is warranted; to date, their current conclusion is that there is insufficient evidence and that further study is warranted (128). Based on the rapid advances in noninvasive carotid artery imaging and plaque characterization, further study of carotid artery imaging's role is also warranted. In the future, risk score systems based on those imaging features need to be developed, evaluated and validated. Randomized clinical trials will investigate whether such approaches provide any incremental clinical information beyond standard luminal assessments.

Acknowledgments

Funding: None.

Footnote

Provenance and Peer Review: This article was commissioned by the Guest Editor (Luca Saba) for the series "Advanced Imaging in The Diagnosis of Cardiovascular Diseases" published in *Cardiovascular Diagnosis and Therapy*. The article was sent for external peer review organized by the Guest Editor and the editorial office.

Conflicts of Interest: All authors have completed the ICMJE uniform disclosure form (available at http://dx.doi.org/10.21037/cdt.2020.03.10). The series "Advanced Imaging in The Diagnosis of Cardiovascular Diseases" was commissioned by the editorial office without any funding or sponsorship. LS served as the unpaid Guest Editor of the series and serves as an unpaid editorial board member of *Cardiovascular Diagnosis and Therapy* from July 2019 to June 2021. DF reports grants from Siemens, other from IschemaView Inc., other from Segmed Inc., grants from American Heart Association, grants from NIH, outside the submitted work. MW reports personal fees from Magnetic Insight, Subtle Medical, NOUS, Icometrix, outside the submitted work. The authors have no other conflicts of interest to declare.

Ethical Statement: The authors are accountable for all aspects of the work in ensuring that questions related to the accuracy or integrity of any part of the work are appropriately investigated and resolved.

References

1. Falk E. Pathogenesis of atherosclerosis. J Am Coll Cardiol 2006;47:C7-12.
2. Zavodni AE, Wasserman BA, McClelland RL, et al. Carotid artery plaque morphology and composition in relation to incident cardiovascular events: the Multi-Ethnic Study of Atherosclerosis (MESA). Radiology 2014;271:381-9.
3. Sun J, Zhao XQ, Balu N, et al. Carotid Plaque Lipid Content and Fibrous Cap Status Predict Systemic CV Outcomes: The MRI Substudy in AIM-HIGH. JACC Cardiovasc Imaging 2017;10:241-9.
4. Saba L, Yuan C, Hatsukami TS, et al. Carotid Artery Wall Imaging: Perspective and Guidelines from the ASNR Vessel Wall Imaging Study Group and Expert Consensus Recommendations of the American Society of Neuroradiology. Am J Neuroradiol 2018;39:E9-31.
5. Schindler A, Schinner R, Altaf N, et al. Prediction of Stroke Risk by Detection of Hemorrhage in Carotid Plaques: Meta-Analysis of Individual Patient Data. JACC

Cardiovasc Imaging 2020;13:395-406.
6. Scoutt LM, Gunabushanam G. Carotid Ultrasound. Radiol Clin North Am 2019;57:501-18.
7. Anzidei M, Napoli A, Zaccagna F, et al. Diagnostic accuracy of colour Doppler ultrasonography, CT angiography and blood-pool-enhanced MR angiography in assessing carotid stenosis: a comparative study with DSA in 170 patients. Radiol Med 2012;117:54-71.
8. Mitchell C, Korcarz CE, Gepner AD, et al. Ultrasound carotid plaque features, cardiovascular disease risk factors and events: The Multi-Ethnic Study of Atherosclerosis. Atherosclerosis 2018;276:195-202.
9. Saba L, Caddeo G, Sanfilippo R, et al. CT and ultrasound in the study of ulcerated carotid plaque compared with surgical results: Potentialities and advantages of multidetector row CT angiography. Am J Neuroradiol 2007;28:1061-6.
10. Etesami M, Hoi Y, Steinman DA, et al. Comparison of carotid plaque ulcer detection using contrast- enhanced and time-of-flight MRA techniques. Am J Neuroradiol 2013;34:177-84.
11. Virmani R, Burke AP, Farb A, et al. Pathology of the vulnerable plaque. J Am Coll Cardiol 2006;47:C13-8.
12. Kwee RM, van Oostenbrugge RJ, Prins MH, et al. Symptomatic patients with mild and moderate carotid stenosis: plaque features at MRI and association with cardiovascular risk factors and statin use. Stroke 2010;41:1389-93.
13. MRC European Carotid Surgery Trial: interim results for symptomatic patients with severe (70-99%) or with mild (0-29%) carotid stenosis. European Carotid Surgery Trialists' Collaborative Group. Lancet 1991;337:1235-43.
14. Redgrave JNE, Lovett JK, Gallagher PJ, et al. Histological assessment of 526 symptomatic carotid plaques in relation to the nature and timing of ischemic symptoms: The Oxford plaque study. Circulation 2006;113:2320-8.
15. Gupta A, Kesavabhotla K, Baradaran H, et al. Plaque echolucency and stroke risk in asymptomatic carotid stenosis: A systematic review and meta-analysis. Stroke 2015;46:91-7.
16. Brinjikji W, Rabinstein AA, Lanzino G, et al. Ultrasound characteristics of symptomatic carotid plaques: A systematic review and meta-analysis. Cerebrovasc. Dis 2015;40:165-74.
17. den Hartog AG, Bovens SM, Koning W, et al. Current status of clinical magnetic resonance imaging for plaque characterisation in patients with carotid artery stenosis. Eur J Vasc Endovasc Surg 2013;45:7-21.
18. Saba L, Saam T, Jäger HR, et al. Imaging biomarkers of vulnerable carotid plaques for stroke risk prediction and their potential clinical implications. Lancet Neurol 2019;18:559-72.
19. Kampschulte A, Ferguson MS, Kerwin WS, et al. Differentiation of intraplaque versus juxtaluminal hemorrhage/thrombus in advanced human carotid atherosclerotic lesions by in vivo magnetic resonance imaging. Circulation 2004;110:3239-44.
20. Takaya N, Yuan C, Chu B, et al. Association between carotid plaque characteristics and subsequent ischemic cerebrovascular events: A prospective assessment with MRI - Initial results. Stroke 2006;37:818-23.
21. Wintermark M, Jawadi SS, Rapp JH, et al. High-resolution CT imaging of carotid artery atherosclerotic plaques. AJNR Am J Neuroradiol 2008;29:875-82.
22. Yim YJ, Choe YH, Ko Y, et al. High signal intensity halo around the carotid artery on maximum intensity projection images of time-of-flight MR angiography: a new sign for intraplaque hemorrhage. J Magn Reson Imaging 2008;27:1341-6.
23. Ajduk M, Pavić L, Bulimbašić S, et al. Multidetector-row computed tomography in evaluation of atherosclerotic carotid plaques complicated with intraplaque hemorrhage. Ann Vasc Surg 2009;23:186-93.
24. Singh N, Moody AR, Gladstone DJ, et al. Moderate carotid artery stenosis: MR imaging-depicted intraplaque hemorrhage predicts risk of cerebrovascular ischemic events in asymptomatic men. Radiology 2009;252:502-8.
25. Ota H, Yu W, Underhill HR, et al. Hemorrhage and large lipid-rich necrotic cores are independently associated with thin or ruptured fibrous caps: An in vivo 3T MRI study. Arterioscler Thromb Vasc Biol 2009;29:1696-701.
26. U-King-Im JM, Fox AJ, Aviv RI, et al. Characterization of carotid plaque hemorrhage: a CT angiography and MR intraplaque hemorrhage study. Stroke 2010;41:1623-9.
27. Saam T, Hetterich H, Hoffmann V, et al. Meta-analysis and systematic review of the predictive value of carotid plaque hemorrhage on cerebrovascular events by magnetic resonance imaging. J Am Coll Cardiol 2013;62:1081-91.
28. Kwee RM, Van Oostenbrugge RJ, Mess WH, et al. MRI of carotid atherosclerosis to identify TIA and stroke patients who are at risk of a recurrence. J Magn Reson Imaging 2013;37:1189-94.
29. Gupta A, Baradaran H, Schweitzer AD, et al. Carotid plaque MRI and stroke risk: a systematic review and meta-analysis. Stroke 2013;44:3071-7.
30. Xu D, Hippe DS, Underhill HR, et al. Prediction of high-

risk plaque development and plaque progression with the carotid atherosclerosis score. JACC Cardiovasc Imaging 2014;7:366-73.
31. Selwaness M, Bos D, Van Den Bouwhuijsen Q, et al. Carotid Atherosclerotic Plaque Characteristics on Magnetic Resonance Imaging Relate with History of Stroke and Coronary Heart Disease. Stroke 2016;47:1542-7.
32. Wang X, Sun J, Zhao X, et al. Ipsilateral plaques display higher T1 signals than contralateral plaques in recently symptomatic patients with bilateral carotid intraplaque hemorrhage. Atherosclerosis 2017;257:78-85.
33. Saba L, Francone M, Bassareo PP, et al. CT attenuation analysis of carotid intraplaque hemorrhage. Am J Neuroradiol 2018;39:131-7.
34. Brinjikji W, DeMarco JK, Shih R, et al. Diagnostic accuracy of a clinical carotid plaque MR protocol using a neurovascular coil compared to a surface coil protocol. J Magn Reson Imaging 2018;48:1264-72.
35. Saba L, Lanzino G, Lucatelli P, et al. Carotid Plaque CTA Analysis in Symptomatic Subjects with Bilateral Intraplaque Hemorrhage: A Preliminary Analysis. Am J Neuroradiol 2019;40:1538-45.
36. Walker LJ, Ismail A, McMeekin W, et al. Computed tomography angiography for the evaluation of carotid atherosclerotic plaque: Correlation with histopathology of endarterectomy specimens. Stroke 2002;33:977-81.
37. Wasserman BA, Smith WI, Trout HH, et al. Carotid artery atherosclerosis: in vivo morphologic characterization with gadolinium-enhanced double-oblique MR imaging initial results. Radiology 2002;223:566-73.
38. Saam T, Ferguson MS, Yarnykh VL, et al. Quantitative evaluation of carotid plaque composition by in vivo MRI. Arterioscler Thromb Vasc Biol 2005;25:234-9.
39. Cai J, Hatsukami TS, Ferguson MS, et al. In vivo quantitative measurement of intact fibrous cap and lipid-rich necrotic core size in atherosclerotic carotid plaque: Comparison of high-resolution, contrast-enhanced magnetic resonance imaging and histology. Circulation 2005;112:3437-44.
40. de Weert TT, Ouhlous M, Meijering E, et al. In vivo characterization and quantification of atherosclerotic carotid plaque components with multidetector computed tomography and histopathological correlation. Arterioscler Thromb Vasc Biol 2006;26:2366-72.
41. Touzé E, Toussaint JF, Coste J, et al. Reproducibility of high-resolution MRI for the identification and the quantification of carotid atherosclerotic plaque components: Consequences for prognosis studies and therapeutic trials. Stroke 2007;38:1812-9.
42. Sun J, Balu N, Hippe DS, et al. Subclinical carotid atherosclerosis: short-term natural history of lipid-rich necrotic core--a multicenter study with MR imaging. Radiology 2013;268:61-8.
43. Sheahan M, Ma X, Paik D, et al. Atherosclerotic Plaque Tissue: Noninvasive Quantitative Assessment of Characteristics with Software-aided Measurements from Conventional CT Angiography. Radiology 2018;286:622-31.
44. Hatsukami TS, Ross R, Polissar NL, et al. Visualization of fibrous cap thickness and rupture in human atherosclerotic carotid plaque in vivo with high-resolution magnetic resonance imaging. Circulation 2000;102:959-64.
45. Yuan C, Zhang SX, Polissar NL, et al. Identification of fibrous cap rupture with magnetic resonance imaging is highly associated with recent transient ischemic attack or stroke. Circulation 2002;105:181-5.
46. Kwee RM, van Engelshoven JMA, Mess WH, et al. Reproducibility of fibrous cap status assessment of carotid artery plaques by contrast-enhanced MRI. Stroke 2009;40:3017-21.
47. Demarco JK, Ota H, Underhill HR, et al. MR carotid plaque imaging and contrast-enhanced MR angiography identifies lesions associated with recent ipsilateral thromboembolic symptoms: An in vivo study at 3T. Am J Neuroradiol 2010;31:1395-402.
48. Trelles M, Eberhardt KM, Buchholz M, et al. CTA for screening of complicated atherosclerotic carotid plaque - American heart association type VI lesions as defined by MRI. Am J Neuroradiol 2013;34:2331-7.
49. Paprottka KJ, Saam D, Rübenthaler J, et al. Prevalence and distribution of calcified nodules in carotid arteries in correlation with clinical symptoms. Radiol Med 2017;122:449-57.
50. Staub D, Patel MB, Tibrewala A, et al. Vasa vasorum and plaque neovascularization on contrast-enhanced carotid ultrasound imaging correlates with cardiovascular disease and past cardiovascular events. Stroke 2010;41:41-7.
51. Huang R, Abdelmoneim SS, Ball CA, et al. Detection of Carotid Atherosclerotic Plaque Neovascularization Using Contrast Enhanced Ultrasound: A Systematic Review and Meta-Analysis of Diagnostic Accuracy Studies. J Am Soc Echocardiogr 2016;29:491-502.
52. Saba L, Lai ML, Montisci R, et al. Association between carotid plaque enhancement shown by multidetector CT angiography and histologically validated microvessel

density. Eur Radiol 2012;22:2237-45.
53. Qiao Y, Etesami M, Astor BC, et al. Carotid plaque neovascularization and hemorrhage detected by MR imaging are associated with recent cerebrovascular ischemic events. Am J Neuroradiol 2012;33:755-60.
54. Chowdhury MM, Tarkin JM, Evans NR, et al. 18F-FDG uptake on PET/CT in symptomatic versus asymptomatic carotid disease: a meta-analysis. Eur J Vasc Endovasc Surg 2018;56:172-9.
55. Makris GC, Lavida A, Griffin M, et al. Three-dimensional ultrasound imaging for the evaluation of carotid atherosclerosis. Atherosclerosis 2011;219:377-83.
56. Touboul PJ, Hennerici MG, Meairs S, et al. Mannheim carotid intima-media thickness and plaque consensus (2004–2006–2011). Cerebrovasc Dis 2012;34:290-6.
57. Den Ruijter HM, Peters SA, Anderson TJ, et al. Common carotid intima-media thickness measurements in cardiovascular risk prediction: a meta-analysis. JAMA 2012;308:796-803.
58. Spence JD. Measurement of carotid plaque burden. JAMA Neurol 2015;72:383-4.
59. Inaba Y, Chen JA, Bergmann SR. Carotid plaque, compared with carotid intima-media thickness, more accurately predicts coronary artery disease events: A meta-analysis. Atherosclerosis 2012;220:128-33.
60. Sillesen H, Muntendam P, Adourian A, et al. Carotid plaque burden as a measure of subclinical atherosclerosis: Comparison with other tests for subclinical arterial disease in the high risk plaque bioimage study. JACC Cardiovasc Imaging 2012;5:681-9.
61. Adraktas DD, Tong E, Furtado AD, et al. Evolution of CT Imaging Features of Carotid Atherosclerotic Plaques in a 1-Year Prospective Cohort Study. J Neuroimaging 2014;24:1-6.
62. Saam T, Hatsukami TS, Yarnykh VL, et al. Reader and platform reproducibility for quantitative assessment of carotid atherosclerotic plaque using 1.5T Siemens, Philips, and general electric scanners. J Magn Reson Imaging 2007;26:344-52.
63. Alizadeh Dehnavi R, Doornbos J, Tamsma JT, et al. Assessment of the carotid artery by MRI at 3T: A study on reproducibility. J Magn Reson Imaging 2007;25:1035-43.
64. Vidal A, Bureau Y, Wade T, et al. Scan-rescan and intra-observer variability of magnetic resonance imaging of carotid atherosclerosis at 1.5 T and 3.0 T. Phys Med Biol 2008;53:6821-35.
65. Syed MA, Oshinski JN, Kitchen C, et al. Variability of carotid artery measurements on 3-Tesla MRI and its impact on sample size calculation for clinical research. Int. J Cardiovasc Imaging 2009;25:581-9.
66. Luo Y, Polissar N, Han C, et al. Accuracy and uniqueness of three in vivo measurements of atherosclerotic carotid plaque morphology with black blood MRI. Magn Reson Med 2003;50:75-82.
67. Sun J, Zhao XQ, Balu N, et al. Carotid magnetic resonance imaging for monitoring atherosclerotic plaque progression: a multicenter reproducibility study. Int. J. Cardiovasc. Imaging 2015;31:95-103.
68. Michel JB, Delbosc S, Ho-Tin-Noé B, et al. From intraplaque haemorrhages to plaque vulnerability: biological consequences of intraplaque haemorrhages. J Cardiovasc Med (Hagerstown) 2012;13:628-34.
69. Hellings WE, Peeters W, Moll FL, et al. Composition of carotid atherosclerotic plaque is associated with cardiovascular outcome: A prognostic study. Circulation 2010;121:1941-50.
70. Eisenmenger LB, Aldred BW, Kim SE, et al. Prediction of Carotid Intraplaque Hemorrhage Using Adventitial Calcification and Plaque Thickness on CTA. AJNR Am J Neuroradiol 2016;37:1496-503.
71. Singh N, Moody AR, Roifman I, et al. Advanced MRI for carotid plaque imaging. Int J Cardiovasc Imaging 2016;32:83-9.
72. Chu B, Hatsukami TS, Polissar NL, et al. Determination of carotid artery atherosclerotic lesion type and distribution in hypercholesterolemic patients with moderate carotid stenosis using noninvasive magnetic resonance imaging. Stroke 2004;35:2444-8.
73. Cai JM, Hatsukami TS, Ferguson MS, et al. Classification of human carotid atherosclerotic lesions with in vivo multicontrast magnetic resonance imaging. Circulation 2002;106:1368-73.
74. Kim SE, Roberts JA, Eisenmenger LB, et al. Motion-insensitive carotid intraplaque hemorrhage imaging using 3D inversion recovery preparation stack of stars (IR-prep SOS) technique. J Magn Reson Imaging 2017;45:410-7.
75. Griffin MB, Kyriacou E, Pattichis C, et al. Juxtaluminal hypoechoic area in ultrasonic images of carotid plaques and hemispheric symptoms. J Vasc Surg 2010;52:69-76.
76. Kakkos SK, Griffin MB, Nicolaides AN, et al. The size of juxtaluminal hypoechoic area in ultrasound images of asymptomatic carotid plaques predicts the occurrence of stroke. J Vasc Surg 2013;57:609-618.e1; discussion 617-8.
77. Redgrave JN, Gallagher P, Lovett JK, et al. Critical cap thickness and rupture in symptomatic carotid plaques: The oxford plaque study. Stroke 2008;39:1722-9.

78. Waki H, Masuyama T, Mori H, et al. Ultrasonic Tissue Characterization of the Atherosclerotic Carotid Artery. Circ J 2003;67:1013-6.
79. Huibers A, De Borst GJ, Wan S, et al. Non-invasive carotid artery imaging to identify the vulnerable plaque: Current status and future goals. Eur J Vasc Endovasc Surg 2015;50:563-72.
80. Sztajzel R, Momjian S, Momjian-Mayor I, et al. Stratified gray-scale median analysis and color mapping of the carotid plaque: Correlation with endarterectomy specimen histology of 28 patients. Stroke 2005;36:741-5.
81. Meissner OA, Rieger J, Rieber J, et al. High-resolution MR imaging of human atherosclerotic femoral arteries in vivo: Validation with intravascular ultrasound. J Vasc Interv Radiol 2003;14:227-31.
82. Virmani R, Kolodgie FD, Burke AP, et al. Lessons From Sudden Coronary Death. Arterioscler Thromb Vasc Biol 2000;20:1262-75.
83. Mauriello A, Sangiorgi GM, Virmani R, et al. A pathobiologic link between risk factors profile and morphological markers of carotid instability. Atherosclerosis 2010;208:572-80.
84. Mosleh W, Adib K, Natdanai P, et al. High-risk carotid plaques identified by CT-angiogram can predict acute myocardial infarction. Int J Cardiovasc Imaging 2017;33:561-8.
85. Spagnoli LG, Mauriello A, Sangiorgi G, et al. Extracranial thrombotically active carotid plaque as a risk factor for ischemic stroke. JAMA 2004;292:1845-52.
86. Moreno PR, Purushothaman KR, Fuster V, et al. Plaque neovascularization is increased in ruptured atherosclerotic lesions of human aorta: Implications for plaque vulnerability. Circulation 2004;110:2032-8.
87. Xiong L, Deng YB, Zhu Y, et al. Correlation of carotid plaque neovascularization detected by using contrast-enhanced US with clinical symptoms. Radiology 2009;251:583-9.
88. Owen DR, Shalhoub J, Miller S, et al. Inflammation within carotid atherosclerotic plaque: Assessment with late-phase contrast-enhanced US. Radiology 2010;255:638-44.
89. Yuan J, Makris G, Patterson A, et al. Relationship between carotid plaque surface morphology and perfusion: a 3D DCE-MRI study. MAGMA 2018;31:191-9.
90. Kerwin W, Hooker A, Spilker M, et al. Quantitative magnetic resonance imaging analysis of neovasculature volume in carotid atherosclerotic plaque. Circulation 2003;107:851-6.
91. Kerwin WS, O'Brien KD, Ferguson MS, et al. Plaque enhancement 2006 Carotid_plaque inflammation in carotid artery. Radiology 2006;241:459-68.
92. Gaens ME, Backes WH, Rozel S, et al. Dynamic contrast-enhanced MR imaging of carotid atherosclerotic plaque: Model selection, reproducibility, and validation. Radiology 2013;266:271-9.
93. Tang T, Howarth SPS, Miller SR, et al. Assessment of inflammatory burden contralateral to the symptomatic carotid stenosis using high-resolution ultrasmall, superparamagnetic iron oxide-enhanced MRI. Stroke 2006;37:2266-70.
94. Smits LP, Tiessens F, Zheng KH, et al. Evaluation of ultrasmall superparamagnetic iron-oxide (USPIO) enhanced MRI with ferumoxytol to quantify arterial wall inflammation. Atherosclerosis 2017;263:211-8.
95. Liu J, Kerwin WS, Caldwell JH, et al. High resolution FDG-microPET of carotid atherosclerosis: plaque components underlying enhanced FDG uptake. Int J Cardiovasc Imaging 2016;32:145-52.
96. Hyafil F, Schindler A, Sepp D, et al. High-risk plaque features can be detected in non-stenotic carotid plaques of patients with ischaemic stroke classified as cryptogenic using combined 18 F-FDG PET/MR imaging. Eur J Nucl Med Mol Imaging 2016;43:270-9.
97. Pirro M, Simental-Mendía L, Bianconi V, et al. Effect of Statin Therapy on Arterial Wall Inflammation Based on 18F-FDG PET/CT: A Systematic Review and Meta-Analysis of Interventional Studies. J Clin Med 2019;8:118.
98. Kim JM, Lee ES, Park KY, et al. Comparison of [18F]-FDG and [18F]-NaF Positron Emission Tomography on Culprit Carotid Atherosclerosis: A Prospective Study. JACC Cardiovasc Imaging 2019;12:370-2.
99. Johnsrud K, Skagen K, Seierstad T, et al. 18 F-FDG PET/CT for the quantification of inflammation in large carotid artery plaques. J Nucl Cardiol 2019;26:883-93.
100. Irkle A, Vesey AT, Lewis DY, et al. Identifying active vascular microcalcification by 18 F-sodium fluoride positron emission tomography. Nat Commun 2015;6:7495.
101. Rosenberg N, Yasin N, Veenman L, et al. 18 kDa Translocator Protein in Mitochondria-Related Pathology: The Case of Traumatic Brain Injury. In: Taskin E, Guven C, Sevgiler Y. editors. Mitochondrial Diseases. 2018:227.
102. Tarkin JM, Joshi FR, Evans NR, et al. Detection of Atherosclerotic Inflammation by 68Ga-DOTATATE PET Compared to [18F]FDG PET Imaging. J Am Coll Cardiol 2017;69:1774-91.
103. Hossain MM, AlMuhanna K, Zhao L, et al. Semiautomatic segmentation of atherosclerotic carotid artery wall volume

using 3D ultrasound imaging. Med Phys 2015;42:2029-43.
104. Zhang Q, Li C, Zhou M, et al. Quantification of carotid plaque elasticity and intraplaque neovascularization using contrast-enhanced ultrasound and image registration-based elastography. Ultrasonics 2015;62:253-62.
105. Roy Cardinal MH, Heusinkveld MHG, Qin Z, et al. Carotid Artery Plaque Vulnerability Assessment Using Noninvasive Ultrasound Elastography: Validation With MRI. AJR Am J Roentgenol 2017;209:142-51.
106. Xie Y, Yu W, Fan Z, et al. High resolution 3D diffusion cardiovascular magnetic resonance of carotid vessel wall to detect lipid core without contrast media. J Cardiovasc Magn Reson 2014;16:67.
107. Zhu DC, Vu AT, Ota H, et al. An optimized 3D spoiled gradient recalled echo pulse sequence for hemorrhage assessment using inversion recovery and multiple echoes (3D SHINE) for carotid plaque imaging. Magn Reson Med 2010;64:1341-51.
108. Wang J, Börnert P, Zhao H, et al. Simultaneous noncontrast angiography and intraplaque hemorrhage (SNAP) imaging for carotid atherosclerotic disease evaluation. Magn Reson Med 2013;69:337-45.
109. Fan Z, Yu W, Xie Y, et al. Multi-contrast atherosclerosis characterization (MATCH) of carotid plaque with a single 5-min scan: technical development and clinical feasibility. J Cardiovasc Magn Reson 2014;16:53.
110. Qi H, Sun J, Qiao H, et al. Carotid intraplaque hemorrhage imaging with quantitative vessel wall T1 mapping: technical development and initial experience. Radiology 2018;287:276-84.
111. Hemmati H, Kamli-Asl A, Talebpour A, et al. Semi-automatic 3D segmentation of carotid lumen in contrast-enhanced computed tomography angiography images. Phys Med 2015;31:1098-104.
112. Diab HMH, Rasmussen LM, Duvnjak S, et al. Computed tomography scan based prediction of the vulnerable carotid plaque. BMC Med Imaging 2017;17:61.
113. Wintermark M, Glastonbury C, Tong E, et al. Semi-automated computer assessment of the degree of carotid artery stenosis compares favorably to visual evaluation. J Neurol Sci 2008;269:74-9.
114. Zhu G, Li Y, Ding V, et al. Semiautomated Characterization of Carotid Artery Plaque Features From Computed Tomography Angiography to Predict Atherosclerotic Cardiovascular Disease Risk Score. J Comput Assist Tomogr 2019;43:452-9.
115. Lekadir K, Galimzianova A, Betriu A, et al. A convolutional neural network for automatic characterization of plaque composition in carotid ultrasound. IEEE J Biomed Health Inform 2017;21:48-55.
116. Banchhor SK, Londhe ND, Araki T, et al. Calcium detection, its quantification, and grayscale morphology-based risk stratification using machine learning in multimodality big data coronary and carotid scans: A review. Comput Biol Med 2018;101:184-98.
117. Saba L, Biswas M, Kuppili V, et al. The present and future of deep learning in radiology. Eur J Radiol 2019;114:14-24.
118. Bhatnagar P, Wickramasinghe K, Williams J, et al. The epidemiology of cardiovascular disease in the UK 2014. Heart 2015;101:1182-9.
119. Benjamin EJ, Muntner P, Alonso A, et al. Heart Disease and Stroke Statistics-2019 Update: A Report From the American Heart Association. Circulation 2019;139:e56-528.
120. Goff DC, Lloyd-Jones DM, Bennett G, et al. 2013 ACC/AHA guideline on the assessment of cardiovascular risk: A report of the American college of cardiology/American heart association task force on practice guidelines. J Am Coll Cardiol 2014;63:2935-59.
121. Garg N, Muduli SK, Kapoor A, et al. Comparison of different cardiovascular risk score calculators for cardiovascular risk prediction and guideline recommended statin uses. Indian Heart J 2017;69:458-63.
122. Li Y, Zhu G, Ding V, et al. Assessing the Relationship between American Heart Association Atherosclerotic Cardiovascular Disease Risk Score and Carotid Artery Imaging Findings. J Comput Assist Tomogr 2018;42:898-905.
123. Gobardhan SN, Dimitriu-Leen AC, van Rosendael AR, et al. Prevalence by Computed Tomographic Angiography of Coronary Plaques in South Asian and White Patients With Type 2 Diabetes Mellitus at Low and High Risk Using Four Cardiovascular Risk Scores (UKPDS, FRS, ASCVD, and JBS3). Am J Cardiol 2017;119:705-11.
124. Grundy SM, Stone NJ, Bailey AL, et al. 2018 AHA/ACC/AACVPR/AAPA/ABC/ACPM/ADA/AGS/APhA/ASPC/NLA/PCNA guideline on the management of blood cholesterol: a report of the American College of Cardiology/American Heart Association Task Force on Clinical Practice Guidelines. J Am Coll Cardiol 2019;73:e285-350.
125. Blaha MJ, Cainzos-Achirica M, Greenland P, et al. Role of Coronary Artery Calcium Score of Zero and Other Negative Risk Markers for Cardiovascular Disease : the Multi-Ethnic Study of Atherosclerosis (MESA). Circulation 2016;133:849-58.

126. Greenland P, Blaha MJ, Budoff MJ, et al. Coronary Calcium Score and Cardiovascular Risk. J Am. Coll Cardiol 2018;72:434-47.
127. Li Y, Zhu G, Ding V, et al. Carotid Artery Imaging Is More Strongly Associated With the 10-Year Atherosclerotic Cardiovascular Disease Score Than Coronary Artery Imaging. J Comput Assist Tomogr 2019;43:679-85.
128. Curry SJ, Krist AH, Owens DK, et al. Risk assessment for cardiovascular disease with nontraditional risk factors: US preventive services task force recommendation statement. JAMA 2018;320:272-80.
129. Zuo HJ, Song XT, Wang JW, et al. A risk score for carotid plaque as an assessment risk of cardiovascular risk among patients with hypertension. J Am Soc Hypertens 2018;12:833-40.
130. Hirata T, Arai Y, Takayama M, et al. Carotid plaque score and risk of cardiovascular mortality in the oldest old: Results from the TOOTH study. J Atheroscler Thromb 2018;25:55-64.
131. Tada H, Nakagawa T, Okada H, et al. Clinical Impact of Carotid Plaque Score rather than Carotid Intima-Media Thickness on Recurrence of Atherosclerotic Cardiovascular Disease Events. J Atheroscler Thromb 2020;27:38-46.
132. Gepner AD, Young R, Delaney JA, et al. Comparison of carotid plaque score and coronary artery calcium score for predicting cardiovascular disease events: The multi-ethnic study of atherosclerosis. J Am Heart Assoc 2017. doi: 10.1161/JAHA.116.005179.
133. Adams A, Bojara W, Schunk K. Early Diagnosis and Treatment of Coronary Heart Disease in Asymptomatic Subjects With Advanced Vascular Atherosclerosis of the Carotid Artery (Type III and IV b Findings Using Ultrasound) and Risk Factors. Cardiol Res 2018;9:22-7.
134. Khanna NN, Jamthikar AD, Gupta D, et al. Effect of carotid image-based phenotypes on cardiovascular risk calculator: AECRS1.0. Med Biol Eng Comput 2019;57:1553-66.
135. Franceschini N, Giambartolomei C, de Vries PS, et al. GWAS and colocalization analyses implicate carotid intima-media thickness and carotid plaque loci in cardiovascular outcomes. Nat Commun 2018;9:5141.
136. Elkoustaf RA, Aldaas OM, Batiste CD, Mercer A, Patterson H, Ismail MH. Lifestyle Interventions and Carotid Plaque Burden: A Comparative Analysis of Two Lifestyle Intervention Programs in Patients with Coronary Artery Disease. Perm J 2019. doi: 10.7812/TPP/18.196.
137. Genkel VV, Kuznetsova AS, Sumerkina VS, et al. The prognostic value of various carotid ultrasound parameters in patients at high and very high cardiovascular risk. Int J Cardiol 2019;292:225-9.
138. Lee CJ, Park S. The role of carotid ultrasound for cardiovascular risk stratification beyond traditional risk factors. Yonsei Med J 2014;55:551-7.
139. Ikeda N, Kogame N, Iijima R, et al. Carotid artery intima-media thickness and plaque score can predict the SYNTAX score. Eur Heart J 2012;33:113-9.

Cite this article as: Zhu G, Hom J, Li Y, Jiang B, Rodriguez F, Fleischmann D, Saloner D, Porcu M, Zhang Y, Saba L, Wintermark M. Carotid plaque imaging and the risk of atherosclerotic cardiovascular disease. Cardiovasc Diagn Ther 2020;10(4):1048-1067. doi: 10.21037/cdt.2020.03.10

